J Appl Electrochem (2013) 43:289–300
DOI 10.1007/s10800-012-0518-x

ORIGINAL PAPER

Effects of organic additives on zinc electrodeposition from alkaline electrolytes

José Luis Ortiz-Aparicio · Yunny Meas · Gabriel Trejo · Raúl Ortega · Thomas W. Chapman · Eric Chainet

Received: 20 September 2012 / Accepted: 11 December 2012 / Published online: 19 December 2012

Abstract This work reports the effects of four organic compounds (referred to as levelers) on the electrodeposition of Zn on steel from alkaline free-cyanide electrolytes. The additives tested included polyvinylalcohol (PVA) and the condensation products of epichlorhydrin with amines, called polyamines (PAs), that were synthesized using an aliphatic amine (PA-I, from diethylamine and PA-II from diethylamine-triethylamine), and a heterocyclic quaternary imidazolium molecule (PA-Imid, from imidazole). These compounds were evaluated in the absence and in addition to a quaternary ammonium brightener, *N*-benzyl-3-carboxylpyridinium chloride (3NCP). The imidazole derivative-based polyamine (PA-Imid) causes greater inhibition of the zinc reduction process than the aliphatic polyamine, and more cathodic overpotential is necessary to promote massive metal deposition. The morphology of the deposits is modified when polyamines are added to the bath; more compact and smaller crystals are obtained with PVA as well as with polyamine PA-I. The addition of PA-II as well as PA-Imid yields crystals growing perpendicular to the substrate. The addition of 3NCP with PVA, PA, or PA-Imid increased the deposition overpotential and modified the morphology by diminishing the grain size. In the absence of additives, crystallographic orientation favored the basal Zn(002) with high atomic packing. The addition of the levelers favored the high-angle pyramidal Zn(101) with low atomic packing. The combination of the levelers with (3NCP) favored the prismatic Zn(100) crystallographic orientation. Additives decrease the size of zinc crystals and tend to increase the energy of lattice favoring the growth of pyramidal and prismatic planes.

Keywords Zinc electrodeposition · Organic additives · Poliamines · Quaternary ammonium brightener

J. L. Ortiz-Aparicio · Y. Meas (✉) · G. Trejo · R. Ortega · T. W. Chapman
Centro de Investigación y Desarrollo Tecnológico en Electroquímica, S. C. Parque Tecnológico Querétaro, Sanfandila, 76703 Pedro Escobedo, Querétaro, Mexico
e-mail: yunnymeas@cideteq.mx

Present Address:
J. L. Ortiz-Aparicio
Centro Nacional de Metrología, Carretera a los Cués, Km 4,5, 75246 El Marqués, Querétaro, Mexico

E. Chainet
Laboratoire d′Electrochimie et Physico-Chimie des Matériaux et Interfaces, (UMR 5631 CNRS-Grenoble INP-UJF), PHELMA BP75, 38402 Saint Martin d′Hères, France

1 Introduction

Zn electrodeposits have been used as a sacrificial protective layer, which retards the corrosion of ferrous substrates [1]. Many efforts have been made to improve the properties of such deposits by studying the effects of the experimental conditions for deposition, such as the electrochemical parameters and the composition of the electrolytes, among others [2, 3]. The presence of additives is an important factor that promotes adequate industrial deposits [3, 4]. Additives are often organic compounds that when added to the plating bath in small amounts are able to modify the crystal growth, thus changing the properties of the deposits. The effects of additives on Zn electrodeposition from alkaline zincate baths have been reported in the literature [5–8]. Additives are often classified as brighteners or levelers, which are known to exert different effects on metal electrodeposition, but the mechanism of action of these compounds is still a matter of study. Brighteners in general

consist of small molecules with specific functional groups whereas levelers are often polymeric or macromolecular compounds. These polymeric additives, also called carriers [1], are used to promote the deposition on sites with low current density, such as cavities.

The use of synthetic Quaternary Ammonium Compounds (QACs) permitted the development of modern alkaline free-cyanide zinc electrolytes [9]. The first reference concerning the application a polyamine (PA) in alkaline zinc plating baths was reported by Winters [10]; this additive was developed to stabilize the alkaline cyanide electrolyte. In addition, due to their stability, QACs have been used as substitutes for polyvinyl alcohol [9]. They have been used in many plating formulations but present some inconvenient effects, such as salting out [1, 9]. Many other complex PAs have been synthesized to improve cyanide [11, 12] and free-cyanide based electrolytes [13–16], being reported earlier in patent literature.

Some fundamental studies have been performed on the action of additives. Macromolecules, often used in metal plating, inhibit the dendritic growth due to their adsorption on electroactive surface sites, thus leveling the rate of deposition [9, 17–30]. Previous studies showed important effects of a PA on the electrochemical and physical characteristics of Zn deposits [17]. Loshkarov et al. [18], using differential capacitance measurements, identified the adsorption of tetraalkylammonium polymers during Zn electrodeposition. Selivanov et al. [19] observed that the zinc reduction process is diffusion controlled without the additive but changed to surface control in the presence of polyethylenepolyamine. Titova et al. [20, 21] showed that macromolecular amines and tetraalkylammonium compounds adsorb on the electrode surface and change the electrochemical mechanism during the nucleation and electrodeposition of Zn from instantaneous to a progressive mechanism [20, 21]. Kryshtop et al. [22] performed a galvanostatic study of nucleation of zinc in the absence and in the presence of a polymeric tetraalkylammonium salt. The authors indicate that the nucleation process occurs in two steps. A product of the condensation reaction between DL-alanine and glutaraldehyde has been used in alkaline zinc plating formulations as a brightening additive [23]. Kavitha et al. [24] studied the effects of carbonyl compounds and their condensation products with semicarbazide on zinc plating; they obtained fine-grained deposits with the latter. Important changes in morphology due to the nature and characteristics of aliphatic and heterocyclic aromatic polyamines were obtained in alkaline Zn plating [25]. Titova et al. studied the effects of a polyamine on ZnFe electrodeposition [26]. Roev et al. [27] found that the structure of the polymer influences the electrodeposition of ZnNi from alkaline baths. Other condensation products were used in ZnNi electrodeposition [28, 29], yielding fine-grained deposits with improved corrosion resistance. It was found that combination of PAs improves the electrochemical behavior, morphology, and crystallographic structure of ZnCo deposits [30].

Other QACs have been used as additives. For example, N-benzyl-3-carboxylpyridinium chloride sodium salt (3NCP) has been studied in alkaline electrolytes [30–33]. In a previous study [39] the effects of different QACs on the electrochemical behavior of electrodeposition as well as on the morphological and crystallographic characteristics of the ZnCo deposits obtained were reported. The effects depend strongly on the chemical structure of the additives [25, 34]. In addition, aliphatic QACs have been shown to prevent dendritic growth; their influence depends on the alkyl chain length [35, 36].

This work continues the previous studies concerning the effects of the chemical structure of additives and its role on Zinc and Zinc alloys electrodeposition [30, 34]. Three polyamines were synthesized varying the nature of the monomer: two aliphatic polyamines (PA-I and PA-II) and a heterocyclic aromatic imidazolium polyamine (PA-Imid) were chosen due to their differences on electron density. Polyvinyl alcohol (PVA) was also studied as a reference polymeric compound. Electrochemical studies were performed, as well as the morphological and crystallographic characterizations of deposits. The presumable chemical structures of additives 3NCP, PVA, PA-I, PA-II, and PA-Imid are presented in Fig. 1. It is expected that the addition of aromatic ring on PA-Imid enhances the interaction with the metal substrate [37]. On the other hand, PVA and PA-I and PA-II do not contain π-bonds. The electrochemical, crystallographic, and morphological behavior with combinations with 3NCP will also be evaluated.

2 Experimental

Electrodeposits were formed from 0.25 M $ZnCl_2$ (Merck). All the solutions were prepared with deionized water (18 MΩ cm). The Zn coatings were electrodeposited on a steel AISI 1018 substrate. The Zn electrolyte base solution is S_0: 0.25 mol/L $ZnCl_2$ + 4.0 mol/L NaOH. Additives used were: Polyvinyl alcohol (Fluka 4–88, MW ~31,000). The polyamine PA-I is the condensation product of the reaction of diethanolamine, epichlorhydrine, and water in a relation in mol 2:1:2. The mixture was refluxed during 8 h until no different phases were observed. Polyamine PA-II was synthesized from PA-I, (from the reaction of diethanolamine, epichlorhydrine, water, and triethylamine (2:1:2:2)) by refluxing the PA-I with triethylamine during 4 h. The condensation products were dissolved in 50 mL of total aqueous solution. The imidazole-polyamine (PA-Imid) was synthesized from the reaction between

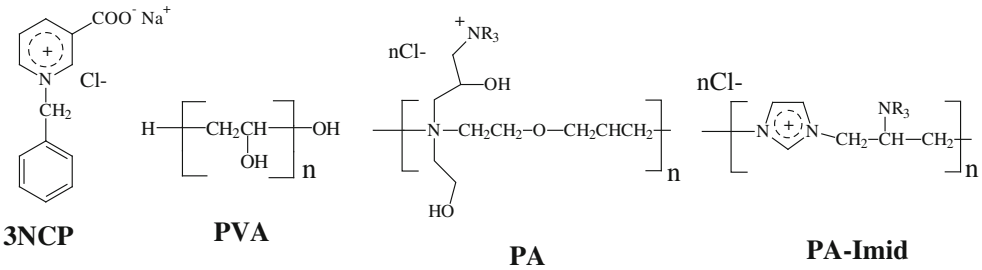

Fig. 1 Chemical structures of the organic quaternary ammonium compounds used as Quaternary Ammonium additives

imidazole, epichlorhydrin, trimethylamine, and water in a relation in mol of 2:1:1:2. The mixture of imidazole, epichlorhydrin, and water was refluxed during 4 h; being the reaction product refluxed in the presence of triethylamine during 4 h, cooled, and dissolved in 50 mL with deionized water. Additive 3NCP was synthesized from the condensation reaction of equivalent molar amounts of benzyl chloride (Aldrich) and nicotinic acid (Aldrich) sodium salt.

The electrochemical experiments were performed with a Potentiostat/Galvanostat Autolab (PGSTAT 30). Cyclic and linear voltammetry were carried out in a typical three electrodes cell. AISI 1018 steel embedded in a Teflon [poly(tetrafluoroethylene)] rod was used as a working electrode with a geometrical area of 0.032 cm^2, a saturated calomel electrode (SCE) was the reference electrode, and the counter electrode was a graphite bar. The trials were carried out under an ultrapure nitrogen atmosphere. Before each experiment, the steel electrode was polished with alumina of 0.05 μm (Buehler) until having a mirror surface appearance. Before the electrodeposition of the coatings, the electrodes were ultrasonically cleaned, etched in 2 % sulfuric acid for 10 s., and rinsed with distilled water. The solution was maintained at ambient temperature.

The morphologies of Zn deposits were examined by scanning electronic microscopy (SEM) (JEOL DSM-5400 LV). The X-rays diffraction experiments were performed in a Brucker X-ray diffractometer (D8 advance) using Cu Kα radiation (λ = 0.15405 nm) and a 2θ scan from 30° to 100°.

3 Results and discussion

3.1 Electrochemical characterization

Bockris et al. [38] and Hendrix et al. [39] suggested that the sequence of zinc reduction reactions (1)–(4) takes place in highly alkaline baths on a zinc electrode, reaction (2) being the rate determining step:

$$Zn(OH)_4^{2-} \rightarrow Zn(OH)_3^- + OH^- \quad (1)$$

$$Zn(OH)_3^- + e^- \rightarrow Zn(OH)_2^- + OH^- \quad (2)$$

$$Zn(OH)_2^- \rightarrow Zn(OH) + OH^- \quad (3)$$

$$Zn(OH) + e^- \rightarrow Zn(0) + OH^- \quad (4)$$

At high current densities, reaction (2) is faster than the incorporation of the Zn adatoms into the growing homogeneous lattice of zinc, producing dendritic and non-adherent deposits [9]. Bright deposits should be obtained if the rate of reaction (2) is reduced [9]. For example, the presence of cyanide ions not only forms complexes with Zn, but its presence controls the rate of reaction (3). The formation of $[Zn(OH)_4]^{2-}$ and $[Zn(CN)_4]^{2-}$ is possible in zincate cyanide baths [2, 9] and, given the overall formation constants values, log β_4: 14.7 and 19, respectively [40], the $[Zn(CN)_4]^{2-}$ complex seems to form quantitatively. However, earlier studies indicate that the reduction of Zn(II) from cyanide-zincate solutions occurs via the formation of $Zn(OH)_2$ intermediate species [41]. Recent studies suggested that interfacial intermediates are formed during the electrodeposition process due to the slow kinetics of zinc–cyanide complex formation [42]. The cyanide ions act not only as a complexing agent but also as a grain refiner during the metal discharge.

A similar mechanism was proposed for PVA [9]; it is considered that this additive forms an adsorbed barrier that controls the rate of reaction (2), which is represented by reactions (5) and (6). According to this assumption, reaction (3) is retarded even more because decomplexation reaction (6) is slow and Zn(I) is somewhat stabilized. On this basis, Darken assumed that the QACs act in a similar way as PVA during zinc electrodeposition [9].

$$PVA + Zn(OH)_3^- + 1e^- \rightarrow [Zn(OH)_2PVA]^- + OH^- \quad (5)$$

$$[Zn(OH)_2(PVA)]^- \rightarrow Zn(OH) + PVA + OH^- \quad (6)$$

Diggle and Damjanovic [35] suggested that two processes may occur when QACs are added in Zn plating baths: the inhibitor could block the electrode, or it could modify the electrode kinetics parameters, changing the diffuse layer due to the specific adsorption on the cations and modifying the location of the reaction plane, i.e., modifying the Helmholtz double layer. These layers are released from the surface at more negative potentials where massive zinc deposition occurs. It must be considered that the metal-electrolyte

interface is a dynamic and complex system. According to Avaca et al. [43], ordered arrangements of cations and anions are able to form on the interface. As the negative charge increases, the anions close to the electrode are repelled, and a cationic monolayer remains on the surface. Such changes, as well as others like electrochemical reactions of additives, can permit the discharge of Zn(II) ions.

3.1.1 Voltammetric study

Cyclic voltammetry studies were performed in order to obtain information about the effects of the additives on zinc electrodeposition, the results are presented in Fig. 2. In the absence of additives (Fig. 2, line a) two small reduction signals (H and H') appear in the potential range previous to massive Zn deposition are observed at −1.12 and −1.34 V versus SCE, respectively (the amplification of the small currents is presented in Inset of Fig. 2). These small signals can be attributed to the reduction of iron oxides and/or hydroxides formed on the surface [44–46]. On the other hand, it is known from previous studies that the evolution reaction is often involved in electrodeposition of metals; the presence of zinc ions in the solution supresses this simultaneous reaction due to the underpotential deposition (upd) of zinc on the iron substrate [47–50]. It is also known that electrokinetic parameters of this reaction vary with the nature of the substrate; the HER is faster on metals like cobalt, iron, and nickel, whereas it is slower on zinc. Therefore, complex events can occur at less cathodic potentials prior to massive zinc reduction: iron oxides and/or hydroxides are able to form on the steel electrode as well as Zn upd which can inhibit the HER to a certain extent. At more negative potentials a single reduction process is observed (peak Ic) at −1.61 V vs SCE. This peak is due to the massive electrodeposition of Zn on the carbon steel electrode. On switching the potential scan direction, a single oxidation peak appears (Ia) attributed to the oxidation of the deposit formed previously.

From previous spectroscopic [51] and thermodynamic [52] studies it was suggested that $Zn(OH)_4^{2-}$ is the predominant Zn species in alkaline solution. Thus, the overall electrochemical reduction during the electrodeposition of the metal may be written as reaction 7:

$$Zn(OH)_4^{2-} + 2e^- \rightarrow Zn + 4OH^- \quad (7)$$

Titova et al. [20] classified cationic quaternary ammonium surfactants into two groups: macromolecular amines obtained from the reaction between heterocyclic amines and epichlorhydrine and tetraalkylammonium salts that involve aliphatic amines. Both types of additive suppress zinc reduction which on a platinum electrode

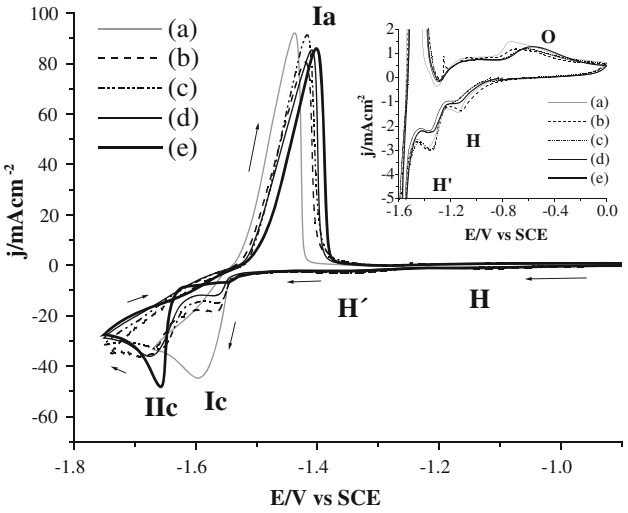

Fig. 2 Ciclic voltammograms for solution S_0 **a** without additives, **b** S_0 + 0.1 g/L PVA, **c** S_0 + 10 mL/L PA-I, **d** S_0 + 10 mL/L PA-II, **e** S_0 + 2 mL/L PA-Imid. Inset: amplification of the voltammograms recorded from solution S_0 without and with the additives. $v = 20$ mV s^{-1}. S_0: 0.25 mol/L $ZnCl_2$ + 4 mol/L NaOH

leads to two consecutive reduction steps [20, 21]. Similar observations were made by Krishtop et al. [22] for zinc electrodeposition on a pyrolitic carbon electrode.

The incorporation of 3NCP in the bath inhibits slightly the reduction peak Ic. This inhibition is often attributed to the partial adsorption of the additive on active surface [4]. When the potential scan is reversed to positive values, the oxidation peak Ia, attributed to the stripping of the zinc deposit previously formed, appears without modifications.

The addition of the polymeric compounds (PVA, PA-I, PA-II, and PA-Imid) changes the cathodic profiles of the voltammograms as can be seen when PVA is added to the electrolyte. Two successive cathodic processes take place (Ic and IIc). The former occurs in the potential range where massive zinc reduction occurs in the absence of additives; this first reduction occurs on the free active surface. Additional deposition on the remainder of the surface requires additional overpotential to drive the reaction. This behavior has been associated with the blocking effect of active sites on the electrode due to the presence of the organic compound in the plating bath [4]. This can be explained if adsorption of the polymer onto the electrode surface partially blocks the active electrode surface. Therefore, a second cathodic peak (IIc) appears at more negative values while the additive desorbs from the electrode surface. With a further increase in the potential to negative values, an increase of the HER, a concomitant process in metal electrodeposition, was observed. Such behavior could be attributed to the increase of the overpotential due o the formation of the organic layer on the

electrode surface. Anodic stripping shows the peak Ia practically without modifications. Similar results were obtained by other authors for Zn [19–22] and for ZnNi [27] electrodeposition from alkaline electrolytes.

The addition of PA-I and PA-II to the electrolyte also modifies the reduction process in a similar way, producing two consecutive reduction peaks (Ic and IIc) in the voltammogram in Fig. 2. The first occurs on the free active area whereas the second (IIc) requires more energy to promote the electrodeposition of zinc. When the potential scan is inverted, a single oxidation is still observed; this indicates that the oxidation process is not affected by the additive (see Fig. 2).

The presence of the imidazole derivative (PA-Imid) changes the electrochemical behavior of zinc plating bath even more (see Fig. 2, line e); a small reduction wave appears around the potential where peak Ic appears, but a larger reduction peak appears at more cathodic potentials (IIc) with a more pronounced *j-E* slope, which indicates a greater degree of surface-site blocking with this additive. Two crossover potentials are observed during the anodic scan. These are associated with nucleation processes [53, 54]. At more positive potentials the usual single oxidation peak appears. It is noted, however, that anodic peak Ia shifts to more positive potentials, which indicates some retardation of the oxidation process by the additive (Fig. 2).

The signals H and H' decrease with the addition of PA-I, PA-II, and with PA-Imid but increase slightly when PVA is added to the electrolyte (Fig. 2). These effects could indicate some interactions of the condensation products with the electrode surface that partially inhibit iron oxide/hydroxide formation. A major characteristic of polymers is their poly-dispersity, with a large number of configurations and a number of points of attachments [3]. Further studies should be done to understand the effects of the polymeric compounds on oxide formation as well as on the Zn upd. The interest in the present work is limited to the influence of these compounds on massive metal electrodeposition.

Adsorption of organic molecules depends on several factors such as the nature of the substrate, the electronic density of the molecules and, therefore, the interaction of molecular orbitals of molecules with those of the substrate, the interactions between water molecules and the electrode surface, as well as water-organic molecule interactions [37]. Two different voltammetric profiles are observed for Zn reduction when the chemical structure of the organic additive varies (Fig. 2). Previous studies indicated that aliphatic [16, 18, 20] and heterocyclic compounds [55] are able to adsorb on electrodes. It must be considered that the cationic nature of these additives may promote adsorption on a negatively charged electrode. Thus, the observed electrochemical changes may be related to different energies of adsorption. Consequently, aromatic groups seem to adsorb preferentially on metallic surfaces.

3.1.2 *Effect of the combination of PVA and polyamines with 3NCP*

Previous studies have shown that combining additives affect the properties of the deposits obtained [56–63]. The results obtained are often different from those obtained with the individual components. In general, the addition of combinations of compounds can decrease the grain size and increase the corrosion resistance of the coatings [56–63]. Figure 3 presents the effects of adding combinations of the polymers (PVA, PA-I, PA-II, and PA-Imid) with 3NCP on the cyclic voltammograms obtained with solution S_0. The results indicate that the additive 3NCP slightly diminishes the cathodic signals.

In the presence of PVA, Fig. 3a, zinc electrodeposition takes place through two consecutive reduction steps. The addition of 3NCP does not modify peak Ic, and the shape of the voltammograms is similar to that obtained in the presence of the polymer alone but with peak IIc diminished. It is possible to infer that some interaction occurs between PVA and 3NCP such that the effects are manifested in the region where desorption of the polymer occurs. The electrolyte with aliphatic polyamines (PA-I and PA-II) gives similar results (Fig. 3b); the diminution of peak IIc indicates a decrease of the metal discharge rate and may be attributed to an increment in the amount of the organic barrier on the surface. Figure 3c shows a major effect for the alkaline zinc electrolyte with PA-Imid added. Peak Ic diminishes even more, and peak IIc shifts to more negative potentials. This effect suggests a stronger interaction of the additives with the electrode surface, and greater potential is necessary to provoke the discharge of the metal ions. Polymeric additives exert the main effect on the electrochemical behavior, and an important partial inhibition occurs on peak IIc. Furthermore, the addition of a polymeric additive and 3NCP increases the HER process as can be seen in the cathodic behavior in Fig. 3.

According to some authors [4], levelers diminish the rugosity of the growing surface, adsorbing on the peaks which tend to have greater current densities. Then, compact deposits and a leveled surface are obtained. The addition of 3NCP presents little effect but when it is added in combination with other additives, the electrochemical characteristics as well as the morphology change markedly. Geduld [1] and Winnand [2] indicated that these polymeric compounds help to dissolve the brighteners in the plating bath. In this way, the barrier formed on the electrode probably increases the interfacial concentration of 3NCP. Then, the chemical identity of the synthesized derivatives plays a role on the effect of the electroreduction of zinc.

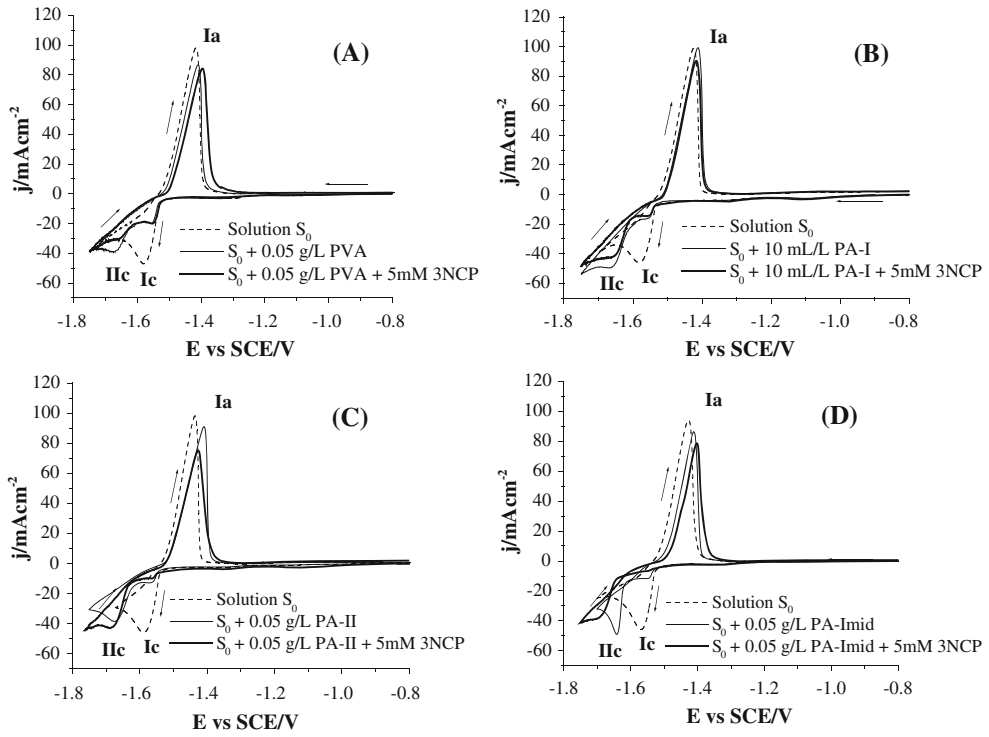

Fig. 3 Cyclic voltammograms of Zn electrodeposition from solution S_0 with additives **a** PVA, **b** PA-I, **c** PA-II, **d** PA-Imid, and the effects of combination with additive 3NCP. Concentrations of the additives are depicted in the figures. $v = 20$ mVs^{-1}

These electrochemical studies show that the small molecule 3NCP does not affect the form of the voltammogram of zinc electroreduction. The presence of greater aliphatic molecules such as the levelers PVA, PA-I, and PA-II exerts an important effect, thus indicating the inhibition of the zinc deposition. The addition of a polyaromatic additive (PA-Imid) increases the inhibition of zinc discharge which could be related with the presence of aromatic rings [55]. The combination of additives (PA-Imid+3NCP) enhances the effect of inhibition of Zn electrodeposition, indicating the synergetic effect of a leveler and a brightener.

3.2 Characterization of the deposits

3.2.1 Morphology of the coatings

Previous studies indicate that the experimental conditions affect the crystal growth during electrodeposition thus changing the morphology of the coatings [64–68]. Some authors tried to relate the morphology with the control of the overall deposition process. Winand [66, 67] indicated that the crystalline shapes result from a competition between perpendicular and parallel growth to the substrate. The morphology depends on the current density and on the degree of inhibition due to the presence of, for example, organic additives [56, 63]. If the inhibition increases, the lateral growth speed increases and dense and coherent deposits are obtained [67]. When the current density increases, three-dimensional nucleation is favored and even isolated crystals and/or dendritic growth are able to form [67]. Wang et al. [68] related the morphology with the controlling conditions and proposed five morphological categories: heavy spongy (under diffusion convection control), dendritic (diffusion control), boulder (diffusion and activation control), layer like (activation control), and mossy (mixed charge transfer and nucleation control). These structures are obtained from very high values to very low current density in the order presented.

It is clear that the presence of additives modifies the crystal growth of zinc. To evaluate the influence of the additives, thin layers were electrodeposited on AISI 1018 carbon steel under potentiostatic conditions. Figure 4a shows the morphology of Zn crystals formed with no additives as typical granular hexagonal platelets [34, 63, 65] with sizes around 4 μm that can be described as boulder morphology. This boulder structure indicates that mixed diffusion and activation control takes place during electrodeposition [68], being in accordance with the lateral and vertical competition of the crystals [66, 67]. The presence of 3NCP modifies the shape of the grains (Fig. 4b), leading to granular boulder morphology and forms cubic crystals, with lower sizes that those observed

without additives, indicating an effect of the additive on the growth of zinc crystals.

The addition of PVA changed the morphology and some clusters are obtained on smaller crystals (Fig. 4c). The size of crystals diminishes but the growth of clusters seems to indicate a diffusion controlled condition, probably due to the adsorbed polyamine layer. The additive PA-I diminishes the crystal sizes producing compact deposits with a boulder shape, which have crystals sizes around 1–2 μm (Fig. 4d). The addition of this additive forms a barrier that controls the metal discharge. Deposits obtained in the presence of PA-II showed needle-like morphologies (Fig. 4e); the crystals seem to grow vertically, which would be attributed to the strong lateral blocking effect of this additive. On the other hand, in Fig. 4f, the addition of PA-Imid produces deposits with even smaller needle-like crystals growing perpendicular to the substrate. Such structures suggest a greater effect on zinc electrodeposition, intensifying the vertical crystal growth.

The presence of leveling additives combined with 3NCP modifies the growth of crystals and produces compact and smaller deposits. Intense HER was observed when both additives were present in the bath. In Fig. 4g, the combination of PVA-3NCP shows smaller crystals but some holes are observed, thus indicating the effect of HER. Combined additives PA-I+3NCP and PA-II+3NCP give smoother bright coatings, the surface being free of holes (Fig. 4h). A finer morphology was obtained with PA-II+3NCP, indicating a better control of the deposition process (Fig. 4i). Finally, the combination of PA-Imid+3NCP gives fine-grained deposits (Fig. 4j). These results agree with previous studies [7, 56–60, 63], the combination of additives improves the appearance of the deposits and diminishes the crystal sizes. According to Nayana et al. [63], the addition of a secondary additive

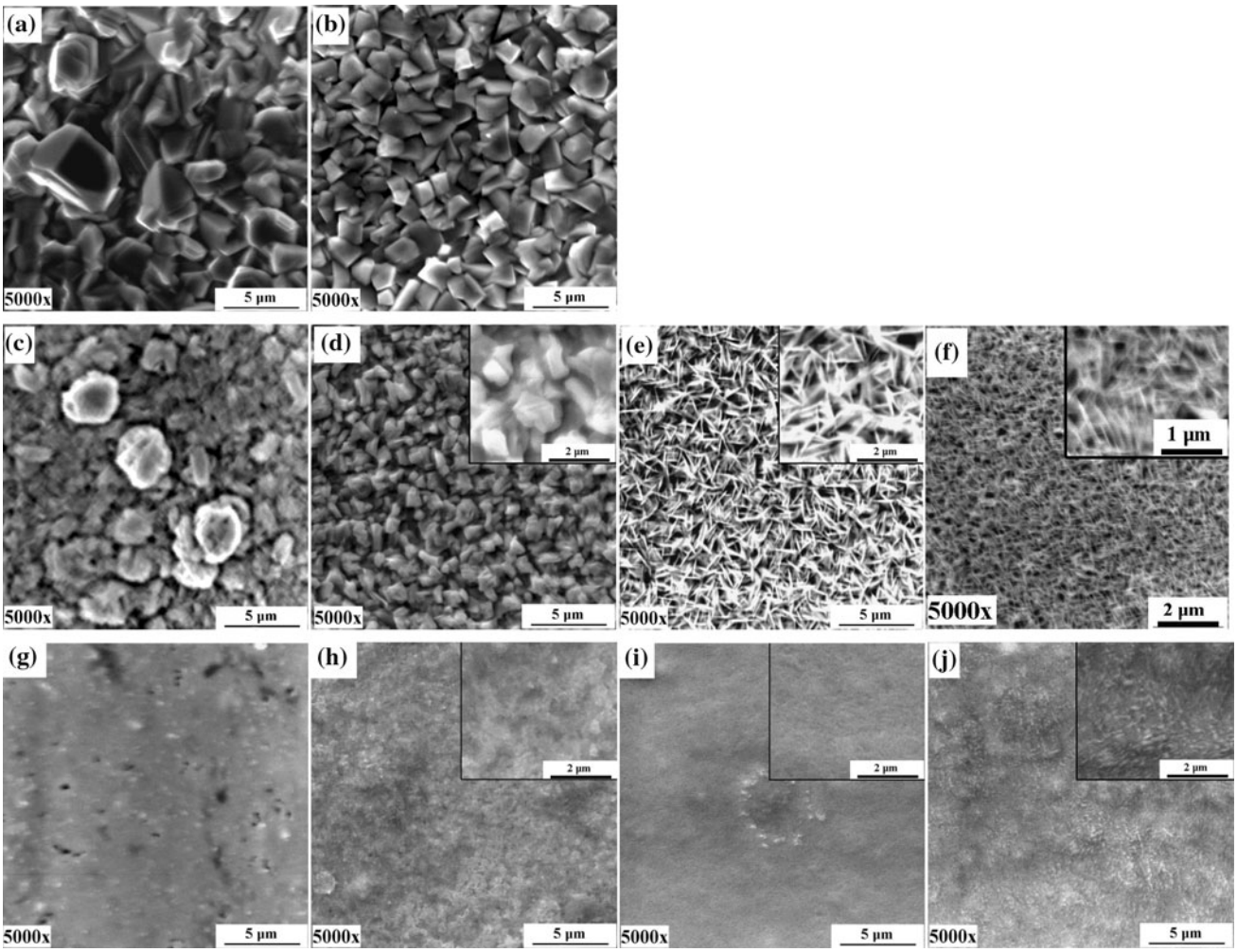

Fig. 4 SEM images of Zn deposits obtained with different electrolytes: **a** solution S_0, **b** S_0 + 5 mM 3NCP, **c** S_0 + 0.1 g/L PVA, **d** S_0 + 10 mL/L PA-I, **e** S_0 + 10 mL/L PA-II, **f** S_0 + 1 mL/L PA-Imid, **g** S_0 + 5 mM 3NCP + 0.1 g/L PVA, (h) S_0 + 5 mM 3*NCP* + 10 mL/LPA-I, **i** S_0 + 5 mM 3NCP + 10 mL/L PA-II, **j** S_0 + 5 mM 3NCP + 1 mL/L PA-Imid. $E_{appl.} = -1.69$ V versus SCE, $t = 180$ s. *Inset*: 10,000x

(brightener) present similar results compared with pure electrolyte without additives; the addition of a primary additive (comprising wetting agents, levelers, and grain refiners) diminishes the nucleation rate and increases the number density of active sites. On the other hand, the addition of combined additives decreases the nucleation rate and increases the number density of active sites even more. Such results agree with the findings observed in the morphology of the thin layers depicted in Fig. 4.

Some theories have been proposed to explain the effects of additives on metal electrodeposition. Additives would adsorb on the interface, inhibiting the electroreduction of metal ions [66]. The electrode kinetics parameters are modified when the inhibitor is adsorbed in the double layer, whereas mass-transport of electroactive species would be affected if the inhibitor interacts in the diffusion layer [66]. Vermilyea [69] suggested that grain refinement is due to the adsorption of species that blocks the propagation of lattice steps during the crystal growth. Kardos and Foulke [70] proposed three mechanisms: diffusion controlled leveling, grain refining, and randomization of crystal growth. Hoar proposed two mechanisms: selective and random [71]. Selective deposition occurs on active sites such as kinks, steps, dislocations, among other surface defects; adsorbed chemical species on the electrode block these favorable sites and impede the free diffusion of adatoms, thus favoring the randomized nucleation of metals, therefore, lateral growth of crystals diminishes and the crystal nuclei density increases. According to some authors [4, 72], leveling additives increase the charge transfer overpotential and, therefore, affect the Tafel parameters. Brighteners primarily reduce the nucleation overpotential and increase secondary nucleation events [72], referred to as 3D nucleation on top of existing grains, increasing the number of active sites on the growing surface and, therefore, the number density of crystals formed [72]. Adcock et al. [72] also pointed out the importance of nucleation overpotential on the formation of fine-grained deposits. Plieth [73] proposed a model, called "local perforation" of the organic film of surfactants, where the presence of brighteners inhibits the complete coverage of the levelers on the electrode surface and allows the transport of metal ions across the film. Natural nucleation and growth are hindered under these conditions, being controlled by the interactions of the organic compounds on the bare substrate as well as the on the growing surface. Such interactions inhibit further growth of formed nuclei but increase the number of new growth centers (with smaller sizes), i.e., increasing the secondary nucleation process.

Bright deposits require that the size of the crystals should be smaller than 0.4 μm, i.e., below the wavelength of visible light [74–76]. Weil and Paquin [74] suggested that brightness and crystallographic orientation of deposits were closely related. However, Denise and Leidheiser [75] did not find a direct relation between brightness and the preferred orientation. Nikolic et al. [76] indicated that the structural characteristics of a bright surface depend on the topographical flat parts, parallel to the surface. These should be closer together to obtain a mirror reflection. They also concluded that no preferential orientation is related to bright surfaces.

From the results presented above, when a combination of additives is added in this alkaline plating bath, very fine grained, smooth, and homogeneous surfaces are obtained. This behavior indicates a synergetic effect of the additives when they are combined. The polymeric compounds act as levelers by diminishing the roughness of the surface while the additive 3NCP acts as a brightener, diminishing the size of the crystals even more. The combination of PVA-3NCP gives fine-grained deposits, but some holes attributed to HER appear on the deposit. The images of deposits obtained in the presence of PA-I, PA-II, and PA-Imid with 3NCP do not present these effects; thus, the polyamines seem to diminish the simultaneous HER. It is interesting to note that the presence of 3NCP alone does not produce bright deposits, but it does when a polyamine is added. Similar results were obtained when polyvinyl alcohol was combined with some aldehydes; these experimental electrolyte conditions produced fine-grained Zn deposits [6, 7]. Our results indicate that microscale leveling (in the order of microns) occurs when PVA, PA-I, PA-II, or PA-Imid are added, and the refinement of crystals is obtained in combinations with 3NCP, which can be viewed as a nanoscale leveling that yields crystals on a nanometric scale when it is in the presence of a leveler, being the result of a synergetic interaction.

3.2.2 *Crystallographic studies*

Experimental conditions maintained during metal electrodeposition, such as temperature, the presence of ions and additives, surface orientation of substrate and others, affect the growth of crystals and, therefore, the orientation of the crystallographic planes [77–82]. Previous studies indicate that the addition of organic additives modifies the diffraction pattern of pure zinc deposits [78–82]. In addition, it is known that the different planes of hexagonal Zn have different energies of formation which depend on the atomic packing [83].

To analyze the preferential orientation of the crystallographic planes of the zinc deposits obtained at different conditions, the texture coefficient was obtained for each orientation. According to the literature, two models have been used to obtain the texture coefficient. Barret and Massalski [84], based on the work of Harris [85], reported a method to calculate the texture coefficient from the relative

intensities of the deposit with respect to the relative intensities of a powder used as a reference, equation 8. This model has been used previously on the study of zinc deposits [86]. Muresan et al. [87] also proposed a method to calculate the texture coefficient, shown in equation 9.

$$T_c(hkl) = \frac{I_{(hkl)}/I_{0(hkl)}}{\frac{1}{n}\sum\left(I_{(hkl)}/I_{0(hkl)}\right)} \quad (8)$$

$$T_c(hkl) = \frac{I_{(hkl)}/I_{0(hkl)}}{\sum I_{(hkl)}/\sum I_{0(hkl)}} \quad (9)$$

where $I_{(hkl)}$ is the relative peak intensity of the zinc electrodeposits, ΣI is the sum of the relative intensities of the independent peaks, and n is the number of reflections. The index 0 denotes the relative intensities for the standard powder sample, in this case the zinc powder relative intensities reported (JPDF 04-0831) was used. The ratio $I_{\mathrm{hkl}}/I_{0(hkl)}$ represents the normalized relative intensities of the reflection of a plane (hkl) of the deposit respect to the same crystallographic orientation of zinc powder. In eq. 8, the expression $(1/n)\Sigma(I_{hkl}/I_{0(hkl)})$ is the average of the normalized relative intensities of the reflections considered. On the other hand, the expression $\Sigma I_{hkl}/\Sigma I_{0(hkl)}$ is the overall normalized relative intensities. In both models, the texture coefficient represents the degree of deviation of the relative intensities with respect to those reported for zinc powder. Figure 5 shows the variation of the texture coefficient (T_c) obtained from the crystallographic diffraction patterns of electrodeposited Zn (Eq. 9) in the absence and with organic additives, according to the method reported by Muresan [87]. Similar results were obtained with the method reported by Harris [85] to describe the preferential crystallographic orientation of the deposits obtained at different conditions.

Without additives, the diffraction pattern of Zn (not shown) was the characteristic reported (JPDF 04-0831). According to Fig. 5, peaks associated with crystallographic pyramidal plane (101), peak of the hexagonal basal plane (002), parallel to the surface, and pyramidal plane (103) are dominant in the massive deposit under the experimental conditions described in Fig. 4a.

Addition of 3NCP affects the crystallographic pattern of the coatings, obtaining a highly oriented deposit where basal peak (002) becomes the most dominant; this indicates that this additive favors the surface parallel growth. The addition of PVA markedly suppresses basal plane (002), increases prismatic (100), and the high-angle pyramidal peak (101) is the dominant orientation (Fig. 5). Similar patterns are still observed when PA-I, PA-II, and PA-Imid are added to the Zn(II) solution (Fig. 5), being pyramidal (101) texture the dominant orientation, followed by prismatic (100). Although the morphology of the deposits differs, the orientation is similar among PVA, PA-I, PA-II, and PA-Imid. These findings indicate that, in general, the macromolecules inhibit parallel growth of the new phase and favor growth of the pyramidal orientation (101) and the prismatic (100) to a minor extent.

The addition of the combination of each macromolecule with 3NCP presents different preferential orientations. The combination of PVA+3NCP increases the prismatic peak (100), and the pyramidal peak (101) presents a similar intensity. Combination of additives PA-I+3NCP gives the peak of prismatic plane (100) the preferred texture. This effect is enhanced when PA-II is used. It can be noted that plane (100) is the dominant plane of the deposit obtained with PA-Imid+3NCP but to a minor extent relative to the combination of PA-II with 3NCP.

According to the results, additives PVA, PA-I, PA-II, and PA-Imid modify the crystallographic orientation, and the high-angle pyramidal peak (101) becomes dominant but not preferential. Then, zinc electrodeposition without additives and with 3NCP favors the formation of the basal (002) plane. Levelers increase the overpotential and favor the formation of high-angle pyramidal low-packing planes. High-energy low-packing prismatic texture of Zn deposits is favored when 3NCP and a leveler are added to the

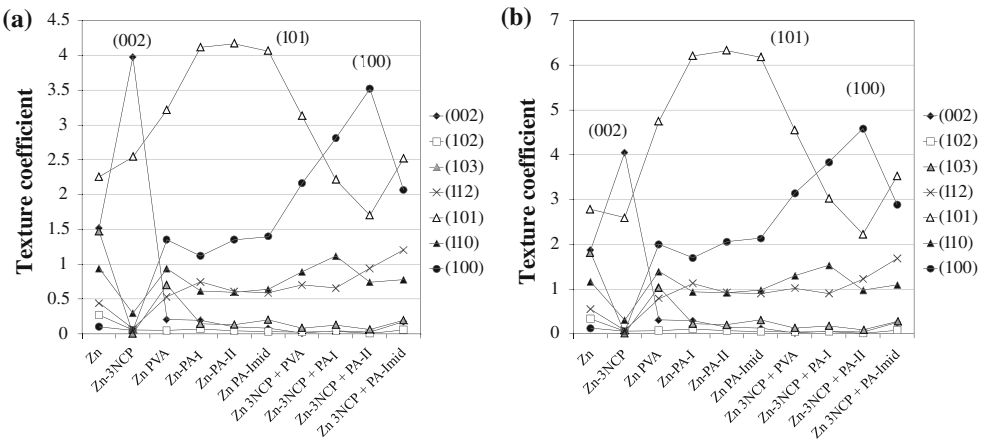

Fig. 5 Variation of the texture coefficient for Zn deposits obtained in the absence and in the presence of organic additives alone and in combination. **a** Method reported by Harris, ref [85], **b** method reported by Muresan et al., ref [87]. Experimental conditions: $E_{\mathrm{appl.}} = -1.69$ V versus SCE, $t = 180$ s

plating solution. Previous studies showed similar results: some additives inhibit the peak of basal plane Zn(002), increasing the prismatic (100) and high-angle pyramidal planes [81]. Nikolic et al. [57, 76] obtained Zn nanocrystals oriented to the prismatic (110) plane using combinations of salicylaldehyde/dextrin. Sato observed the transition of Zn basal (002) and (11.*l*) to prismatic (110) when the concentration of additives increased, high-index pyramidal (112) orientation being a transient preferential orientation at intermediate concentrations [78]. Chandrasekar et al. [7] found the transition from basal Zn (002) plane (obtained without additives) to pyramidal (102) and (112) planes (obtained in the presence of PVA) obtained from alkaline conditions. The addition of piperonal and PVA gives Zn deposits with preferential prismatic (100) and pyramidal (112) planes.

Similar results were obtained in acidic conditions [63]; the preferential (002) basal plane was dominant in the absence of additives, pyramidal (101), prismatic (100) and (110) appear in the presence of single additives. The dominant peak was (100) prismatic plane when combined additives were added to the electrolyte. Therefore, the addition and/or combination of additives are related with changes in the electrochemical behavior, morphology, and texture. As a general trend, the formation of the prismatic planes would be related with the presence of two additives: a brightener and a leveler. From the results of the study performed by Nayana et al. [63], it is possible to analyze the trend of the dominant crystallographic planes in terms of its energy of formation: basal plane (002) dominates in the absence of additives, and pyramidal (101), (102), and (112) are favored with the brightener. The addition of the leveler favors prismatic (110) plane, and finally the combination favors the (100) prismatic plane, which possesses the greater energy of formation.

Some theories have been proposed to explain the factors that influence the preferential texture during electrodeposition. Pangarov [77] suggested that two-dimensional crystal growth (2D) occurs initially, and the orientation is defined by the applied overpotential. Planes with low energy of formation would develop at low overpotentials; then formation of the most closely packed plane Zn(002) is expected. Youssef et al. [82] argued that Pangarov's theory [77] does not account the effects of adsorbed compounds. Reddy suggested that the adsorption rate of foreign substances on growing crystals depends on the crystallographic planes. Planes with little or no adsorption should grow preferentially [88]. Sato indicated that favorable orientations are determined by the growth rate of various crystallographic planes [78], which depend on the degree of interaction of organic compounds with the growing surface. Szeptycka [89] proposed that preferred orientation is the result of the contribution of surface energy and work function of the crystallographic planes, the former increasing in low atomic density planes whereas the second increases at high atomic density arrangements. Li and Szpunar [90, 91] argued that the development of different textures is possible due to differences in the surface energy; some textures are favored because they minimize the surface energy of the system, i.e., the surface anisotropy energy. As the deposit grows, grains having higher surface energy tend to reduce their surface area (*S*), and those with low surface energy increase it [90]. Youssef et al. showed that the preferred orientation of Zn changes with pulse potential [82]. As the applied overpotential increased, the texture of Zn deposits changed in the following way: basal (002) < low-angle pyramidal (104) and (103) planes < high-angle pyramidal (112) and (101) planes < prismatic (110) and (100) orientations (formed at the highest overpotentials). These results were explained in terms of atomic packing; Zn deposition with crystallographic planes having high atomic packing is favored at low overpotentials whereas low atomic packing planes require higher overpotentials [82, 83]. The highest atomic packing plane is basal plane (002), and the lowest atomic packing plane corresponds to prismatic (100). Then, minimization of the surface energy (more specifically the integral $\int \gamma \cdot dS$ because of the surface tension (γ) dependence with crystal planes and direction) is an important factor in the morphology and crystallography of surfaces.

When the interaction between the atoms of the deposit and those of the substrate is relatively strong, the preferred orientation of the growing grains is epitaxial [91]. On the other hand, the epitaxial influence of the substrate is absent when the electrodeposition occurs on an inert substrate, and the texture of the deposits is determined solely by electrodeposition conditions [91]. Ohmori reported the epitaxial growth of Zn onto Fe substrates, which follow specific texture relationships between the Zn deposit and the steel surface, called Burger's orientation relationships [92, 93], namely: Fe(100)//Zn(101), Fe(110)//Zn(002), and Fe(111)//Zn(002). Raeissi et al. [94–96] suggest that differences in the morphology of the substrate have important effects on the growth modes of Zn deposits. On electropolished surfaces, non-epitaxial growth via 3D nucleation of Zn(002) (growing parallel to Fe(110) plane) and epitaxial growth of pyramidal Zn(115) and Zn(116) planes following 2D nucleation were observed. Mechanically polished electrodes favor only pyramidal $Zn(11X)_{3 \leq X \leq 6}$ orientations by intensive 3D nucleation, which is caused by the multiple active sites due to scratches on the surface [95]. In this work, the texture of the carbon steel electrode was identified as a body centered cubic (bcc) α-Fe, (JPDF 06-0696), being Fe(110) the dominant plane. Then, the development of Zn(002) would be favored, being in accordance with previous results [93–97].

Electrochemical results correlate with morphological and crystallographic findings and showed the relation of the chemical nature of the additives on the electrochemical behavior during Zn(II) reduction. Aliphatic PVA and PA gives similar results, i.e., they partially inhibit Zn(II)-ion reduction, and the electrodeposition process occurs in two steps. The addition of PA-Imid enhances the inhibition of peak Ic. Polymeric additives act as levelers that increase the massive-reduction overpotential. This leads to the increment of the vertical and lateral growth rates that are blocked by the additives, which promotes 3D nucleation on top of existing nuclei, producing smaller crystals and compact deposits. Greater overpotentials inhibit high atomic packing plane (002), which is mainly formed by two-dimensional (lateral) nucleation, and favor vertical growth through 3D nucleation, which is in accord with the morphological observations. Additive 3NCP alone produces some changes in the Zn voltammograms and in the shape of crystals. The preferential orientation changes markedly, favoring the formation of the high atomic packing plane, basal plane (002). It was also seen that the addition of 3NCP combined with the polymeric additives increases the overpotential of Zn(II) reduction, diminishes the IIc peak current density values, reduces the size of crystals, and changes the orientation of deposits; a single preferred texture was not observed, but deposits formed were oriented to the high-energy, low atomic packing planes.

4 Conclusions

This work examined the effects of polyamine compounds and the effects of concurrent addition of *N*-benzyl-3-carboxylpyridinium chloride sodium salt (NCP) on alkaline Zn deposition. The addition of PVA or aliphatic PA-I and PA-II modifies the voltammograms in a similar way; the reduction process takes place through two consecutive steps. The first reduction step seems to occur on the free active surface not covered by the additive whereas the second reduction process occurs at greater potentials where desorption of the additives is reached. The addition of the Imidazole derivative PA-Imid suppresses even more the first cathodic reduction and leads to a second cathodic process at more negative potentials. Such behavior is related with the chemical structure of the polyamine. The combination of additives PVA, PA-I, PA-II, and PA-Imid with 3NCP exhibits interactions that inhibit the second reduction process. Synergetic interactions occur that cause fine-grained deposits to be formed.

The presence of additives PVA or PA modifies the morphology of Zn crystals producing compact deposits with a boulder morphology indicating that a mixed diffusion and activation control takes place. With PA-II and PA-Imid, Zn deposits growth perpendicular to the steel substrate, diminishing the crystal sizes. The combination of the PVA and the polyamines with 3NCP result in the formation of very fine-grained crystals with a smooth and bright appearance due to a synergetic effect of both additives. These results were explained in terms of a microscale leveling when PVA, PA-I, PA-II, or PA-Imid are added, and a nanoscale leveling when the polymers are added in the presence of 3NCP, occurring via a "local perforation" mechanism.

The presence of additives also changes the texture of the coatings, being observed a trend of the crystallographic orientations: without additives and with 3NCP alone, the basal Zn(002) crystallographic plane is the dominant orientation. In the presence of PVA and polyamines, the high-index pyramidal plane (101) dominates, and with the combination of the levelers with 3NCP, peak of the high-energy low atomic packing prismatic plane (100) dominates. Therefore, under these experimental conditions, additives decrease the size of zinc crystals and increase the energy of lattice favoring the growth of prismatic planes.

Acknowledgments The authors thank Consejo Nacional de Ciencia y Tecnología (CONACyT), México, Project 31411, for financial assistance. J.L. Ortiz-Aparicio is also grateful for CONACyT scholarships. F. Manriquez is thanked for help in obtaining SEM images.

References

1. Geduld H (1988) Zinc Plating. ASM International, Ohio
2. Winand R (2000) In: Schlessinger M, Paunovic M (eds) Modern electroplating, electrochemical society series. Wiley, New York, p 423
3. Paunovic M, Schlesinger M (1998) Fundamentals of electrochemical deposition. Wiley, New York
4. Oniciu L, Muresan L (1991) J Appl Electrochem 21:565
5. Pereira MS, Barbosa LL, Souza CAC et al (2006) J Appl Electrochem 36:727
6. Chandrasekar MS, Srinivasan S, Pushpavanam M (2010) J Mat Sci 45:1160
7. Chandrasekar MS, Shanmugasigamani, Pushpavanam M (2010) Mat Chem Phys 124:516
8. Rethinam AJ, Ramesh Bapu GNK, Muralidharan VS (2003) Trans Inst Met Finish 81:136
9. Darken J (1979) Trans Inst Met Finish 57:145
10. Winters JB (1957) Method of electrodepositing zinc. US Patent 2,791,554
11. Burnson RH (1966) Alkaline cyanide bath and process for electroplating therewith. US Patent 3,227,638
12. Rosenberg WE (1968) Bright zinc electro-plating. US Patent 3,393,135
13. Rosenberg WE (1974) Composition of baths for electrodeposition of bright zinc. US Patent 3,824,158
14. Creutz HG (1974) Method to improve zinc deposition employing multi-nitrogen quaternaries. US Patent 3,853,718
15. Nobel F and Ostrow BD (1975) Electrolytes for the electrolytic deposition of zinc. US Patent 3,869,358
16. Rushmere JD (1977) Polyamine additives in alkaline zinc electroplating. US Patent 3,824,158

17. Zuñiga V, Ortega R, Meas Y et al (2004) Plat Surf Finísh 91(6):46
18. Loshkaryov YM, Vlinov VM, Gnedenkov LY et al (1989) Bull Electrochem 5:254
19. Selivanov VN, Bobrikova IG, Molchanov SV et al (1997) Russ J Electrochem 33:179
20. Titova VN, Kazakov VA, Yavich AA et al (1996) Russ J Electrochem 32:562
21. Titova VN, Javich AA, Petrova NV et al (2000) Bull Electrochem 16:425
22. Krishtop YG, Yurchenko NP, Trofimenko VV (2007) ECS Trans 6:165
23. Arthoba-Naik Y, Venkatesha TV (2005) Bull Mater Sci 28:495
24. Kavitha B, Santhosh P, Renukadevi M et al (2006) Surf Coat Technol 201:3438
25. Hsieh JC, Hu CC, Lee TC (2009) Surf Coat Technol 203:3111
26. Titova VN, Kazakov VA, Yavich AA, Petrova NV (1999) Russ J Electrochem 35:134
27. Roev VG, Kaidrikov RA, Khakimullin AB (2001) Russ J Electrochem 37:756
28. Li GY, Lian JS, Niu LY, Jiang ZH (2005) Surf Coat Technol 191:59
29. Hosseini MG, Ashassi-Sorkhabi H, Ghiasvand HAY (2008) Surf Coat Technol 202:2897
30. Ortiz-Aparicio JL, Meas Y, Trejo G et al (2009) J Electrochem Soc 156:K205
31. James BS, McWhinnie WR (1980) Trans Inst Met Finish 58:72
32. Mirkova L, Monev M, Krastev I et al (1995) Trans Inst Met Finish 73:107
33. Monev M, Mirkova L, Krastev I et al (1998) J Appl Electrochem 28:1107
34. Ortiz-Aparicio JL, Meas Y, Trejo G et al (2008) J Electrochem Soc 155:D167
35. Diggle JW, Damjanovic A (1972) J Electrochem Soc 119:1649
36. Lan CJ, Lee CY, Chin TS (2007) Electrochim Acta 52:5407
37. Lipkowski J, Ross PN (1992) Adsorption of molecules at metal electrodes. VCH, New York
38. Schrebler-Guzman RS, Vilche JR, Arvìa AJ (1979) Electrochim Acta 24:395
39. Wieckowski A, Ghali E (1985) Electrochim Acta 30:1423
40. Öjefors L (1976) J Electrochem Soc 123:1691
41. Rashkov S, Bozhkov C, Kudryavtsev V et al (1988) J Electroanal Chem 248:421
42. Wijenberg JHOJ, Stevels JT, de Wit JHW (1998) Electrochim Acta 43:649
43. Maleeva EA, Pedan KS (1996) Russ J Electrochem 32:415
44. Maleeva EA, Pedan KS, Ponjomarev II (1996) Russ J Electrochem 32:1380
45. Cain KJ, Melendres CA, Maroni VA (1987) J Electrochem Soc 134:519
46. Zhang Y, Muhammed M (2001) Hydrometallurgy 60:215
47. Fletcher S (1983) Electrochim Acta 28:917
48. Fletcher S, Halliday CS, Gates D et al (1983) J Electroanal Chem 159:267
49. Vyaseleva GY, Sabirov RK, Manyurov IR et al (1997) Russ J Electrochem 33:126
50. Bockris JO'M, Zagy N, Damjanovic A (1972) J Electrochem Soc 119:285
51. Hendrikx J, van Der Putten A, Visscher W et al (1984) Electrochim Acta 29:81
52. Lurie J (1975) Handbook of analytical chemistry. MIR, Moscow
53. Gerisher H (1953) Z Phys Chem 202:302
54. Rezaite V, Vishomirskis R (2001) Prot Met 37:31
55. Avaca LA, González ER, Rúvolo-Filho A (1982) J Appl Electrochem 12:405
56. Martyak NM (2003) Mater Charact 50:269
57. Nikolić N, Rakočević Z, Djurovic DR et al (2006) Russ J Electrochem 42:1121
58. Li MC, Jiang LL, Zhang WQ et al (2007) J Solid State Electrochem 11:549
59. Li M, Luo S, Qian Y et al (2007) J Electrochem Soc 154:D576
60. Youssef KMS, Koch CC, Fedkiw PS (2004) J Electrochem Soc 151:C103
61. Zhang W, Lu X, Liu Y et al (2007) J Electrochem Soc 154:D526
62. Hsieh J, Hu CCC (2008) and Lee TC J. Electrochem Soc 155:D675
63. Nayana KO, Venkatesha TV, Praveen BM et al (2011) J Appl Electrochem 41:39
64. Mansfeld F, Gilman S (1970) J Electrochem Soc 117:588
65. Sonneveld PJ, Visscher W, Barendrecht E (1992) Electrochim Acta 37:1199
66. Winand R (1992) Hydrometallurgy 29:567
67. Winand R (1994) Electrochim Acta 39:1091
68. Wang RY, Kirk DW, Zhang GX (2006) J Electrochem Soc 153:C357
69. Vermilyea DA (1959) J Electrochem Soc 106:66
70. Kardos O, Foulke DG (1962) In: Tobias CW (ed) Advances in electrochemistry and electrochemical engineering, Vol 2. Interscience, New York, p 145
71. Hoar TP (1953) Trans Inst Met Finish 29:7566
72. Adcock PA, Adelju SB, Newman OMG (2002) J Appl Electrochem 32:1101
73. Plieth W (1992) Electrochim Acta 37:2115
74. Weil R, Paquin R (1960) J Electrochem Soc 107:87
75. Denise F, Leidheiser H (1953) J Electrochem Soc 100:490
76. Nikolić ND, Rakočević Z, Popov KI (2001) J Electroanal Chem 514:56
77. Pangarov NA (1965) J Electroanal Chem 9:70
78. Sato R (1959) J Electrochem Soc 106:206
79. Oren Y, Landau U (1982) Electrochim Acta 27:739
80. Mouanga M, Ricq L, Douglade J et al (2007) J Appl Electrochem 37:283
81. Sekar R, Jayakrishnan S (2006) J Appl Electrochem 36:591
82. Youssef KM, Koch CC, Fedkiw PS (2008) Electrochim Acta 54:677
83. Matysina ZA, Chuprina LM, Zaginaichenko SY (1992) J Phys Chem Solids 53:167
84. Barret C, Massalski TB (1980) Structure of metals. Pergamon, Oxford
85. Harris GB (1952) Phil Mag 43:113
86. Khorsand S, Raeissi K, Golozar MA (2011) Corros Sci 53:2676
87. Muresan L, Oniciu L, Froment M, Maurin G (1992) Electrochim Acta 37:2249
88. Reddy AKN (1963) J Electroanal Chem 6:141
89. Szeptycka B (2001) Russ J Electrochem 37:805
90. Li DY, Szpunar JA (1997) Electrochim Acta 42:47
91. Li DY, Szpunar JA (1997) J Mat Sci 32:5513
92. Kozlov VM, Peraldo-Bicelli L (2002) Mat Chem Phys 77:289
93. Kamei K, Ohmori Y (1987) J Appl Electrochem 17:821
94. Ohmori Y, Nakai K, Ohtsubo H et al (1993) ISIJ Int 33:1196
95. Raeissi K, Saatchi A, Golozar MA, Szpunar JA (2004) J Appl Electrochem 34:1249
96. Raeissi K, Saatchi A, Golozar MA, Szpunar JA (2005) Surf Coat Technol 197:229
97. Raeissi K, Bateni MR, Saatchi A et al (2006) Surf Coat Technol 201:3116